AFOSR-86-0167

MF-120

Courant Institute of
Mathematical Sciences

Magneto-Fluid Dynamics Division

# THEORY OF LONG-PERIOD MAGNETIC PULSATIONS

Satoshi Hamaguchi and William Grossmann

Plasma Physics
ember 1989



NEW YORK UNIVERSITY

UNCLASSIFIED

New York University
Courant Institute of Mathematical Sciences
Magneto-Fluid Dynamics Division

MF-120 AFOSR-86-0167

# THEORY OF LONG-PERIOD MAGNETIC PULSATIONS

Satoshi Hamaguchi and William Grossmann

November 1989

# Theory of Long-Period Magnetic Pulsations

SATOSHI HAMAGUCHI* and WILLIAM GROSSMANN
Courant Institute of Mathematical Sciences
251 Mercer Street
New York, New York 10012

**Abstract**

Theories of Alfvén resonance and Kelvin-Helmholtz instability are reviewed to elucidate a possible mechanism of the long-period continuous magnetic pulsations (pc3 ~ pc5).

*Present Address: Institute for Fusion Studies, The University of Texas at Austin, Austin, Texas 78712.

# 1. Introduction

It is now known that the earth's magnetic field fluctuates with a wide range of frequencies. Aside from extremely long time scales associated with the earth's interior physics (such as dipole reversal of the earth's magnetic field), the time scale of the magnetic field fluctuations ranges from several days, caused by magnetic storms, to less than a second, caused by Larmor motion of protons. The temporal changes in the geomagnetic field with the range of periods from fractions of a second to several minutes, with which we are particularly concerned in this review, are called magnetic pulsations. These pulsations have been measured with magnetometers placed on the earth's surface (ground observation) and on space-craft (in-situ observation).

The magnetic pulsations have been known for over a hundred years. Historically such rapid changes in the earth's magnetic field were first reported by B. Stewart in 1861. He reported a large magnetic storm recorded at the Kew Observatory in England. It is shown in this report that the magnitude of the magnetic field fluctuations is of several hundred $\gamma$ ($1\gamma = 10^{-5}$gauss) and their typical time scale is on the order of few minutes. In particular, during the International Geophysical Year (IGY) in 1957–1958 and in the succeeding years, the international collaboration on the earth's geophysical study became established and the global observation of the geomagnetic field variations such as magnetic pulsations began to be made.

Based on such global observation, the earth's magnetic field variations have been classified into categories according to the frequency. One of the simplest and most widely used classifications is based on nine categories according to the regularity and the period. In this classification the pulsations pc1 $\sim$ pc6, which have rather well-defined spectral peaks, are called continuous pulsations while the pulsations pi1 $\sim$ pi3, which have a wide spectral

range, are called irregular pulsations. This is summarized in Table 1, where pc6 and pi3 are not referred to but another kind of classification sc and si is used. A more detailed classification has been proposed by Saito [1976], where time evolution of frequency of each pulsation is also taken into account (Table 2). In the short period range for pc1 and pi1, the subclassification based on the time evolution of frequencies is considered to be particularly important.

The detailed mechanism of the variations of the earth's magnetic field has not been understood completely as yet. However, it is widely believed that the pc pulsations (in particular pc3 $\sim$ pc5) are caused by the resonant oscillations of the earth's magnetic field lines since they have distinctive periodicity. Because of the high conductivity of the ionosphere, the shear Alfvén wave traveling along the magnetic field line is expected to be reflected at the intersection of the field line and the ionosphere and a standing wave will be excited on the field line (field line resonance). Therefore, the fundamental period of the oscillation is given by

$$T = 2 \int \frac{ds}{v_A}, \tag{1.1}$$

where $v_A$ denotes the Alfvén velocity and the integration is to be taken between the two conjugate points along a given field line. Therefore the period given by Eq. (1.1) depends on geomagnetic latitude or the $L$-value of the field line. Figure 1 shows how the period is expected to vary with latitude if Eq. (1.1) holds for every field line [Saito, 1976].

This simple theory of the field line resonance, however, does not bear out the observation that the pulsation with the same frequency is often recorded simultaneously over a latitude range of several degrees [Hirasawa, 1970; Samson and Rostoker, 1972]. Indeed, as we will show in Sec. 2, field lines having different eigenfrequencies can be coupled together and oscillate as a mass. Therefore the period given by Eq. (1.1) does not necessarily indicate the observed period of magnetic pulsations and some other mechanism may be responsible to make certain spectral peaks stand out in the pc spectrum. It is now believed that there

are basically two types of mechanisms causing spectral peaks in the pc oscillations. One mechanism is an external one, namely a monochromatic oscillation is excited away from the resonant field line, probably outside or at the boundary of the magnetosphere, and then it is transmitted toward the earth as a compressional wave and resonates on a field line. One of the most prominent candidates for the external wave source is the Kelvin-Helmholtz instability, which is expected to occur at the magnetopause or the boundary between the solar wind in the magnetosheath and the plasma in the magnetosphere. Once such a monochromatic wave propagates in the magnetosphere, Alfvén waves are excited in response to the source wave in the region where the eigenperiod of the geomagnetic field line coincides with the period of the source wave. This mechanism is called Alfvén resonance and due to the nonuniformity of the magnetic fields. This phenomenon has been applied to many situations in laboratory and space and astrophysical plasmas over the past twenty years [Tataronis and Grossmann, 1973; Grossmann and Tataronis, 1973; and Hameiri and Hammer, 1979].

The other mechanism which might be responsible for the spectral peaks in the magnetic pulsations is an internal one, namely excitation of a monochromatic wave occurs inside the magnetosphere. One of the widely accepted theories of this mechanism is excitation of the surface wave on the surface where the Alfvén velocity changes abruptly [Chen and Hasegawa, 1974b]. This mechanism explains plasma-pause associated magnetic pulsations (the frequency of which falls into pc3 $\sim$ pc5), which are weakly damped coherent oscillations at $L \simeq 3$ and are accompanied by impulse-like perturbations at $L \simeq 4$ [Lanzerotti et al., 1973].

In this review, we focus on the first mechanism of the pc-pulsations mentioned above [Nishida, 1978; Lanzerotti and Southwood, 1979; Rostoker, 1979; Haerendel and Paschmann, 1982; Southwood and Hughes, 1983]; in particular, the Kelvin-Helmholtz instability is considered as a possible wave source. The rest of this paper is organized as follows. In Sec. 2 the theory of Alfvén resonance is presented. In Sec. 3 the magnetohydrodynamic (MHD)

Kelvin-Helmholtz instability is discussed. The last section contains summary and discussion.

## 2. Resonant Excitation of Alfvén Waves

We now consider the response of the magnetosphere to a monochromatic source wave, assuming that such a source wave may be generated by an instability such as the Kelvin-Helmholtz instability at the magnetopause. A coupling between an active process releasing free energy such as the Kelvin-Helmholtz instability and a passive process such as the resonant excitation of an Alfvén wave (which is observed as geomagnetic pulsations) was first studied by Southwood [1974], using a straight field line model, and also independently by Chen and Hasegawa [1974a], using the dipole field model. In this section, we mainly follow the work of Chen and Hasegawa [1974a] (see also Hasegawa and Chen [1974]).

We assume that the magnetosphere can be described by the ideal MHD equations:

$$\rho \frac{d}{dt}\mathbf{v} = -\nabla p + (\nabla \times \mathbf{B}) \times \mathbf{B}, \tag{2.1a}$$

$$\frac{\partial \mathbf{B}}{\partial t} = \nabla \times (\mathbf{v} \times \mathbf{B}), \tag{2.1b}$$

$$\frac{dp}{dt} + \gamma p \nabla \cdot \mathbf{v} = 0, \tag{2.1c}$$

where

$$\frac{d}{dt} = \frac{\partial}{\partial t} + \mathbf{v} \cdot \nabla, \tag{2.1d}$$

$$\nabla \cdot \mathbf{B} = 0, \tag{2.1e}$$

and

$$p = A\rho^{\gamma}. \tag{2.1f}$$

Here $\rho$, $p$, $\mathbf{B}$, and $\mathbf{v}$ denote the mass density, the pressure, the magnetic field, and the velocity field, respectively, $\gamma$ denotes the ratio of the specific heats, and $A$ is a constant. We write each dependent variable as a sum of the time-independent mean part, denoted by subscript 0, and the small fluctuating part, denoted by subscript 1. For example, $\mathbf{B} = \mathbf{B}_0 + \mathbf{B}_1$. Assuming that the mean fluid velocity vanishes, we write $\mathbf{v}\,(= \mathbf{v}_1)$ as the fluctuating fluid velocity. Since the following linearized equations do not involve the fluctuating mass density, we write $\rho\,(= \rho_0)$ as the mean part of the mass density.

Assuming that the mean quantities $\mathbf{B}_0$, $p_0$, and $\rho$ are zeroth order quantities while the fluctuating quantities are first order quantities, we linearize the system (2.1):

$$\rho\ddot{\boldsymbol{\xi}} = -\nabla\left(p_1 + \mathbf{B}_0 \cdot \mathbf{B}_1\right) + \left(\mathbf{B}_1 \cdot \nabla\right)\mathbf{B}_0 + \left(\mathbf{B}_0 \cdot \nabla\right)\mathbf{B}_1 \tag{2.2a}$$

$$\mathbf{B}_1 = -\mathbf{B}_0(\nabla \cdot \boldsymbol{\xi}) + \left(\mathbf{B}_0 \cdot \nabla\right)\boldsymbol{\xi} - (\boldsymbol{\xi} \cdot \nabla)\mathbf{B}_0 \tag{2.2b}$$

$$p_1 = -(\boldsymbol{\xi} \cdot \nabla)p_0 - \gamma p_0(\nabla \cdot \boldsymbol{\xi}), \tag{2.2c}$$

where $\boldsymbol{\xi}$ denotes the plasma displacement, defined by $\dot{\boldsymbol{\xi}} \equiv \mathbf{v}$ and the equilibrium condition $\nabla p_0 = (\nabla \times \mathbf{B}_0) \times \mathbf{B}_0$ is used. Substituting Eq. (2.2b) into Eq. (2.2a), we obtain

$$\rho\ddot{\boldsymbol{\xi}} - \left(\mathbf{B}_0 \cdot \nabla\right)^2 \boldsymbol{\xi} = -\nabla\left(p_1 + \mathbf{B}_0 \cdot \mathbf{B}_1\right) + \mathbf{C}, \tag{2.3}$$

where

$$\mathbf{C} = -\left(\mathbf{B}_0 \cdot \nabla\right)\left\{(\boldsymbol{\xi} \cdot \nabla)\mathbf{B}_0 + \mathbf{B}_0(\nabla \cdot \boldsymbol{\xi})\right\} + \left(\mathbf{B}_1 \cdot \nabla\right)\mathbf{B}_0. \tag{2.4}$$

We note here that the dispersion relation of the shear Alfvén wave is given by

$$\rho\ddot{\boldsymbol{\xi}}_\perp - \left(\mathbf{B}_0 \cdot \nabla\right)^2 \boldsymbol{\xi}_\perp = 0$$

and the dispersion relation of the surface wave excited by the Kelvin-Helmholtz instability in an incompressible plasma is given by [Sen, 1963]

$$\nabla^2\left(p_1 + \mathbf{B}_0 \cdot \mathbf{B}_1\right) = 0,$$

which will be shown in Sec. 3 [Eq. (3.5)]. Thus Eq. (2.3) represents a coupling between the shear Alfvén wave and the surface Alfvén wave with the strength of the coupling being determined by C.

In order to solve the system of equations (2.2c), (2.3), and (2.4) in a special case, we now assume a simple geometry. Suppose all mean quantities depend only upon the $y$-coordinate, the straight magnetic field line is in the $z$-direction and all fluctuating quantities depend on time and space in a form $f(y)\exp i\left(k_\perp x + k_\parallel z - \omega t\right)$, we obtain

$$\frac{d}{dy}\left(\frac{\varepsilon\alpha B^2}{\varepsilon - \alpha B^2 k_\perp^2}\frac{d\xi_y}{dy}\right) + \varepsilon\xi_y = 0 \tag{2.5}$$

from Eqs. (2.2c), (2.3), and (2.4). In this geometry, the $y$-direction represents the radially outward direction in the actual magnetosphere, the $z$-direction represents the south-north direction and the $x$-direction represents the east-west direction. In Eq. (2.5), $\xi_y$ is the $y$-component of $\xi$,

$$\begin{aligned}
\varepsilon(y) &= \omega^2\rho(y) - k_\parallel^2 B^2(y), \\
\alpha(y) &= 1 + \gamma\beta + \frac{\gamma\beta^2 k_\parallel^2 B^2}{\omega^2\rho - \gamma\beta k_\parallel^2 B^2}, \\
\beta(y) &= \frac{p_0}{B^2},
\end{aligned}$$

and

$$B \equiv |\mathbf{B}_0|.$$

Furthermore, we assume a wave localized in the east-west direction, i.e., $k_\perp \gg k_\parallel \simeq \omega/v_A$, where $v_A = B/\sqrt{\rho}$ is the Alfvén velocity. Then Eq. (2.5) becomes

$$\frac{d^2\xi_y}{dy^2} + \frac{d\ln\varepsilon}{dy}\frac{d\xi_y}{dy} - k_\perp^2\xi_y = 0, \tag{2.6}$$

where we used $\alpha B^2 k_\perp^2 \gg |\varepsilon|$. For a given source wave frequency $\omega$ (which generally has a small positive imaginary part indicating damping) the position $y_0$ of the resonant field line

is given by the condition $\mathrm{Re}\,\varepsilon\,(y_0) = 0$. Away from the resonant field line, the plasma and the magnetic field are almost homogeneous (i.e., $d\ln\varepsilon/dy \simeq 0$) except for some discontinuity surface such as the magnetopause. In such region, Eq. (2.6) is of the form $\nabla_\perp^2\xi_y = d^2\xi_y/dy^2 - k_\perp^2\xi_y = 0$, which gives the surface wave solution $\xi_y = \hat{\xi}_y \exp\left(-|k_\perp|\,(y - y_d)\right)$. Here $y_d$ denotes the position of the discontinuity surface. The strong coupling of the surface wave and the local Alfvén wave at $y = y_0$ occurs when the discontinuity surface is close to the resonant surface.

Near the resonant field line, we may obtain the solution of Eq. (2.6) by expanding $\varepsilon(y)$ around the resonant point $y_0$

$$\varepsilon(y) = \varepsilon\,(y_0) + \frac{\partial\varepsilon}{\partial y}\bigg|_{y=y_0}(y - y_0)\,.$$

If weak dissipation is present, then the source wave has a small positive imaginary part $\mathrm{Im}\,\omega(\ll \mathrm{Re}\,\omega)$. In this case, $\left|(\varepsilon/\partial\varepsilon/\partial y)_{y=y_0}\right| \simeq \left|(\varepsilon_i/\partial\varepsilon_r/\partial y)_{y=y_0}\right|$ is small compared with a typical scale length of the variation of plasma parameters. Here $\varepsilon_r = \mathrm{Re}\,\varepsilon$ and $\varepsilon_i = \mathrm{Im}\,\varepsilon$. Using the following parameter

$$\gamma' \equiv \frac{\varepsilon_i}{\partial\varepsilon_r/\partial y}\bigg|_{y=y_0},$$

we therefore rewrite Eq. (2.5) near $y_0$ as

$$\frac{d^2\xi_y}{dy^2} + \frac{1}{y - y_0 + i\gamma'}\frac{d\xi_y}{dy} - k_\perp^2\xi_y = 0. \tag{2.7}$$

The Alfvén speed $v_A = B/\sqrt{\rho}$ is believed to be an increasing function of the distance toward the earth (i.e., $y$ in our case) except at the plasma pause. Therefore, the $y$-derivative of $\varepsilon_r$ at $y = y_0$

$$\begin{aligned}\frac{d\varepsilon_r}{dy}\bigg|_{y=y_0} &= \left(\frac{1}{\rho}\frac{d\rho}{dy}\varepsilon_r + \rho\frac{d}{dy}\left(-k_\parallel^2\frac{B^2}{\rho}\right)\right)\bigg|_{y=y_0} \\ &= -\rho\frac{d}{dy}\left(v_A^2 k_\parallel^2\right)\bigg|_{y=y_0}\end{aligned}$$

is negative except at the plasma pause, and so is the parameter $\gamma'$. We note that $k_{||}$ is generally an increasing function of the distance toward the earth, although in our planar geometry $k_{||}$ is a constant.

The solution of Eq. (2.7) is given by

$$\xi_y = CI_0\left(k_\perp\left(y - y_0 + i\gamma'\right)\right) + DK_0\left(k_\perp\left(y - y_0 + i\gamma'\right)\right),$$

where $I_0$ and $K_0$ are modified Bessel functions and $C$ and $D$ are constants. The corresponding eigenmode is shown to be continuous. With a monochromatic wave source, the solution of Eq. (2.7) near $y = y_0$ is approximately given by

$$\xi_y \simeq C\ln(Y - 1 + i\eta), \tag{2.8}$$

where $Y = y/y_0$ and $\eta = \gamma'/y_0$. It can be shown that the wave near the resonant field line $y = y_0$ is noncompressional [Hasegawa and Chen, 1974], as one would expect for a shear Alfvén mode. Therefore the equation $\nabla \cdot \boldsymbol{\xi} = 0$, together with the assumption $k_\perp \gg k_{||}$, yields the expression of the $x$-component of $\xi$ near $y_0$

$$\xi_x \simeq \frac{iC}{k_\perp y_0}\frac{1}{Y - 1 + i\eta}. \tag{2.9}$$

We now discuss the polarization of the wave obtained above. The relationship between $\boldsymbol{\xi}$ and $\mathbf{B}_1$ is given from Eq. (2.2b)

$$\begin{cases} B_{1x} = ik_{||}B_0\xi_x \\ B_{1y} = ik_{||}B_0\xi_y, \end{cases}$$

where the subscripts $x$ and $y$ indicate the $x$ and $y$ components of the associated quantities, respectively. Therefore, near the resonant field line, we obtain from Eqs. (2.8) and (2.9)

$$\begin{aligned} \frac{B_{1x}}{B_{1y}} &= -ik_\perp y_0(Y - 1 + i\eta)\ln(Y - 1 + i\eta) \\ &= g + ih, \end{aligned} \tag{2.10}$$

where

$$g = k_\perp y_0 \left( \frac{\eta}{2} \ln \left( \Delta Y^2 + \eta^2 \right) + \Delta Y \tan^{-1} \frac{\eta}{\Delta Y} \right),$$

$$h = k_\perp y_0 \left( \eta \tan^{-1} \frac{\eta}{\Delta T} - \frac{\Delta Y}{2} \ln \left( \Delta Y^2 + \eta^2 \right) \right),$$

and

$$\Delta Y = Y - 1.$$

Since $\Delta Y \simeq 0$ near the resonant field line, we have

$$g \simeq k_\perp y_0 \frac{\eta}{2} \ln \eta^2$$

$$h \simeq k_\perp y_0 |\eta| \frac{\pi}{2} \operatorname{sign} \Delta Y.$$

The signs of the functions $g$ and $h$ are then given by

$$\operatorname{sign} g = -\operatorname{sign} (k_\perp \eta) \tag{2.11}$$

$$\operatorname{sign} h = \operatorname{sign} (k_\perp \Delta Y) \tag{2.12}$$

since $\eta^2 \ll 1$ or $\ln \eta^2 < 0$. From Eq. (2.10) we have

$$\frac{\operatorname{Re} B_{1x}}{\operatorname{Re} B_{1y}} = g - h \tan \left( k_\perp x + k_\parallel z - (\operatorname{Re} \omega) t \right),$$

so the sense of polarization is determined by the sign of $h$. From Eq. (2.12), it is clear that the sense of polarization switches across the resonant field line at $y = y_0$.

The ellipticity and the angle of polarization can be seen from the equation

$$(\operatorname{Re} B_{1y})^2 - 2g (\operatorname{Re} B_{1y}) (\operatorname{Re} B_{1x}) + \left( g^2 + h^2 \right) (\operatorname{Re} B_{1x})^2 = |B_{1x}|^2 h^2, \tag{2.13}$$

which is also derived from Eq. (2.10). It is easy to show that the orbit of the point ($\operatorname{Re} B_{1x}$, $\operatorname{Re} B_{1y}$) given by Eq. (2.13) is an ellipse. Solving Eq. (2.13) for $\operatorname{Re} B_{1x}$, we obtain

$$\operatorname{Re} b_y = g (\operatorname{Re} B_{1x}) \pm h \sqrt{|B_{1x}|^2 - (\operatorname{Re} B_{1x})^2}. \tag{2.14}$$

Hence, as one approaches the resonant field line (i.e. $h \to 0$), the ellipticity becomes large and the polarization becomes linear at the resonant field line ($h = 0$). Figure 2 summarizes the angle of polarization obtained from Eq. (2.14). In this figure, $k_\perp$ is written as $m$, $x$ and $y$ are written as $\hat{\phi}$ and $\hat{\nu}$, respectively. Assuming that the monochromatic source wave is generated by the Kelvin-Helmholtz instability at the magnetopause, the sign of $m$ changes across the local noon: $m$ is negative (positive) in the morning (afternoon) side. As shown in Fig. 2, the angle of the polarization switches across the local noon since the sign $g$ changes as the sign of $m$ changes. The amplitude, the ellipticity, and the sense of the polarization of the wave on the morning side ($m < 0$) are shown in Fig. 3. In this figure, the parameter $\nu(= y)$ corresponds to $L$-value, so the horizontal axis also can be viewed as latitude. The change of the sense of the polarization given in Fig. 3 bears out the observation shown in Fig. 4 [Samson et al., 1971].

# 3. Kelvin-Helmholtz Instability

In this section we discuss the Kelvin-Helmholtz instability at the magnetopause, which is considered to be a source of the monochromatic wave that leads to resonant oscillations of the geomagnetic field lines. For simplicity we first ignore the width of the magnetopause. It is also assumed that there is a uniform infinite flow of the magnetized plasma on the magnetosheath side (Side I), whose velocity $\mathbf{v}_0^{(\mathrm{I})}$ is tangential to the magnetopause, and the plasma on the magnetosphere side (Side II) is at rest. Giving a small perturbation to this magnetosheath-magnetosphere boundary model, we will follow the time evolution of the perturbation [Sen, 1963].

We use the incompressible ideal MHD equations, i.e., Eqs. (2.1a), (2.1b), (2.1d), (2.1e), and

$$\nabla \cdot \mathbf{v} = 0, \tag{3.1}$$

together with the boundary conditions

$$v_n - v_s = 0 \tag{3.2a}$$

$$[B_n] = 0 \tag{3.2b}$$

$$\left[p + \frac{B_t^2}{2}\right] = 0. \tag{3.2c}$$

Here the subscripts $n$ and $t$ denote the directions normal and tangential to the discontinuity surface or the magnetopause, respectively, $v_s$ refers to the (normal) velocity of the discontinuity surface and the square bracket is the change in the value of the enclosed expression across the discontinuity. It should be noted that we obtain the boundary conditions (3.2a), (3.2b), and (3.2c) by requiring that Eq. (3.1), $\nabla \cdot \mathbf{B} = 0$ and the normal component of the momentum Eq. (2.1a) hold across the boundary. As in Sec. 2, we write each dependent variable as a sum of the time-independent mean part and the small fluctuating part such as $\mathbf{B} = \mathbf{B}_0 + \mathbf{B}_1$, $\mathrm{v} = \mathbf{v}_0 + \mathbf{v}_1$, and $p = p_0 + p_1$, and then linearize the system of the equations. Here we assume that $p_0 = 0$ on both sides and $\mathbf{v}_0 = 0$ in the magnetosphere (Side II). In order to distinguish the variables on Side I and II, we use superscripts (I) and (II); for example, $B_0^{(\mathrm{I})}$ denotes the mean magnetic field on Side I and $p_1^{(\mathrm{II})}$ denotes the perturbed pressure on Side II. We choose a coordinate system in such a way that the $y$-direction is normal to the discontinuity surface (from the magnetosphere (Side II) to the magnetosheath (Side I)), the $x$-direction is in the direction of the mean flow $\mathbf{v}_0^{(\mathrm{I})}$ in the magnetosheath and the $z$-direction is perpendicular to these two directions (Fig. 5). By linearizing the system of the equations, we obtain

$$\rho^{(i)}\left(\frac{\partial}{\partial t} + \mathbf{v}_0^{(i)} \cdot \nabla\right)\mathbf{v}_1^{(i)} = -\nabla p_1^{(i)} + \left(\nabla \times \mathbf{B}_1^{(ii)}\right) \times \mathbf{B}_0^{(i)}, \tag{3.3a}$$

$$\frac{\partial \mathbf{B}_1^{(i)}}{\partial t} = -\left(\mathbf{v}_0^{(i)} \cdot \nabla\right)\mathbf{B}_1^{(i)} + \left(\mathbf{B}_0^{(i)} \cdot \nabla\right)\mathbf{v}_1^{(i)}, \tag{3.3b}$$

$$\nabla \cdot \mathbf{v}_1^{(i)} = 0, \tag{3.3c}$$

$$\nabla \cdot \mathbf{B}_1^{(i)} = 0, \tag{3.3d}$$

for both fluids $i$ = I and II. As we have assumed, $\mathbf{v}_0^{(i)}$ and $\mathbf{B}_0^{(i)}$ are constant vectors and $\mathbf{v}_0^{(\mathrm{II})} = 0$.

Rewriting the last term of the right-hand side of Eq. (3.3a) as

$$\left(\nabla \times \mathbf{B}_1^{(i)}\right) \times \mathbf{B}_0^{(i)} = -\nabla\left(\mathbf{B}_0^{(i)} \cdot \mathbf{B}_1^{(i)}\right) + \left(\mathbf{B}_0 \cdot \nabla\right)\mathbf{B}_1 \tag{3.4}$$

and taking the divergence of both sides of Eq. (3.3a), we obtain

$$\nabla^2\left(p_1^{(i)} + \mathbf{B}_0^{(i)} \cdot \mathbf{B}_1^{(i)}\right) = 0. \tag{3.5}$$

Applying $\mathbf{B}_0^{(i)}$ to both Eq. (3.3a) and Eq. (3.3b) and eliminating $\mathbf{B}_0 \cdot \mathbf{v}_1^{(i)}$ from the resulting equations yields

$$\rho^{(i)}\left(\frac{\partial}{\partial t} + \mathbf{v}_0^{(i)} \cdot \nabla\right)^2\left(\mathbf{B}_0^{(i)} \cdot \mathbf{B}_1^{(i)}\right) + \left(\mathbf{B}_0^{(i)} \cdot \nabla\right)^2 p_1^{(i)} = 0. \tag{3.6}$$

We now denote the $x$-, $y$-, and $z$-components of $\mathbf{B}_1^{(i)}$ by $B_{1x}^{(i)}$, $B_{1y}^{(i)}$, and $B_{1z}^{(i)}$, respectively. Taking the $y$-component of Eq. (3.3a) and applying $\mathbf{B}_0^{(i)} \cdot \nabla$ to the resulting equation, we obtain

$$\begin{aligned}\rho^{(i)}\left(\frac{\partial}{\partial t} + \mathbf{v}_0^{(i)} \cdot \nabla\right)\left(\mathbf{B}_0^{(i)} \cdot \nabla\right) v_{1y}^{(i)} &= -\frac{\partial}{\partial Z}\left(\mathbf{B}_0^{(i)} \cdot \nabla\right)\left(p_1^{(i)} + \mathbf{B}_0^{(i)} \cdot \mathbf{B}_1^{(i)}\right) \\ &\quad + \left(\mathbf{B}_0^{(i)} \cdot \nabla\right)^2 \mathbf{B}_{1y}^{(i)}.\end{aligned} \tag{3.7}$$

Eliminating $\left(\mathbf{B}_0^{(i)} \cdot \nabla\right) v_{1y}^{(i)}$ from the $y$-component of Eq. (3.3b) and Eq. (3.7) yields

$$\rho^{(i)}\left\{\left(\frac{\partial}{\partial t} + \mathbf{v}_0^{(i)} \cdot \nabla\right)^2 - \left(\mathbf{B}_0^{(i)} \cdot \nabla\right)^2\right\} B_{1y}^{(i)} + \frac{\partial}{\partial Z}\left(\mathbf{B}_0^{(i)} \cdot \nabla\right)\left(p + \mathbf{B}_0^{(i)} \cdot \mathbf{B}_1^{(i)}\right) = 0. \tag{3.8}$$

Integrating Eq. (3.3b) for $i$ = II in time at $y = 0$, we obtain

$$\mathbf{B}_1^{(\mathrm{II})} - \left(\mathbf{B}_0^{(\mathrm{II})} \cdot \nabla\right)\xi = 0, \tag{3.9}$$

where $\xi$ denotes the infinitesimal displacement of the discontinuity surface (Fig. 5a). From the boundary conditions (3.2a) and (3.2b), the similar equation holds for Side I at $y = 0$;

$$\mathbf{B}_1^{(\mathrm{I})} - \left(\mathbf{B}_0^{(\mathrm{I})} \cdot \nabla\right) \xi \;=\; 0. \tag{3.10}$$

From Eq. (3.5), we also have

$$[p_1 + \mathbf{B}_0 \cdot \mathbf{B}_1] = 0. \tag{3.11}$$

We now consider the normal mode solutions of this linearized system, assuming that all dependent variables have the following dependence on $t$, $\mathbf{r} = (x, z)$ and $y$:

$$\begin{aligned} &\exp i\,(\omega t - (\mathbf{k} \cdot \mathbf{r}) - \gamma_1 y) \quad \text{in fluid (I)} \quad (y > 0) \\ &\exp i\,(\omega t - (\mathbf{k} \cdot \mathbf{r}) + \gamma_2 y) \quad \text{in fluid (II)} \quad (y < 0), \end{aligned} \tag{3.12}$$

where $\mathbf{k}$ is the propagation vector, $\omega$ is the complex frequency, and $\gamma_1$ and $\gamma_2$ are real positive constants so that the solutions decay as $|y| \to \infty$. The propagation vector $\mathbf{k}$ is taken to be the same in both fluids. From Eq. (3.5), we obtain

$$\gamma_1 = \gamma_2 = k \equiv |\mathbf{k}|. \tag{3.13}$$

Using the dependence given by Eqs. (3.12) and (3.13), we derive the following linear algebraic homogeneous equations in the matrix form:

$$
\begin{bmatrix}
-\left(\mathbf{k}\cdot\mathbf{B}_0^{(\mathrm{I})}\right)^2 & 0 & -\rho^{(\mathrm{I})}(\omega-\mathbf{k}\cdot\mathbf{v}_0)^2 & 0 & 0 & 0 & 0 \\
0 & -\left(\mathbf{k}\cdot\mathbf{B}_0^{(\mathrm{II})}\right)^2 & 0 & -\rho^{(\mathrm{II})}\omega^2 & 0 & 0 & 0 \\
ik\left(\mathbf{k}\cdot B_0^{(\mathrm{I})}\right) & 0 & ik\left(\mathbf{k}\cdot\mathbf{B}_0^{(\mathrm{I})}\right) & 0 & -\rho^{(\mathrm{I})}(\omega-\mathbf{k}\cdot\mathbf{v}_0)^2+\left(\mathbf{k}\cdot B_0^{(\mathrm{I})}\right)^2 & 0 & 0 \\
0 & -ik\left(\mathbf{k}\cdot\mathbf{B}_0^{(\mathrm{II})}\right) & 0 & -ik\left(\mathbf{k}\cdot\mathbf{B}_0^{(\mathrm{II})}\right) & 0 & -\rho^{(\mathrm{II})}\omega^2+\left(\mathbf{k}\cdot\mathbf{B}_0^{(\mathrm{II})}\right)^2 & 0 \\
0 & 0 & 0 & 0 & 1 & 0 & ik\cdot\mathbf{B}_0^{(\mathrm{I})} \\
0 & 0 & 0 & 0 & 0 & 1 & ik\cdot\mathbf{B}_0^{(\mathrm{II})} \\
1 & -1 & 1 & -1 & 0 & 0 & 0
\end{bmatrix}
\begin{bmatrix}
p_1^{(\mathrm{I})} \\
p_1^{(\mathrm{II})} \\
\mathbf{B}_0^{(\mathrm{I})}\cdot\mathbf{B}_1^{(\mathrm{I})} \\
\mathbf{B}_0^{(\mathrm{II})}\cdot\mathbf{B}_1^{(\mathrm{II})} \\
B_{1y}^{(\mathrm{I})} \\
B_{1y}^{(\mathrm{II})} \\
\xi
\end{bmatrix} = 0 \,. \tag{3.14}
$$

Here $\mathbf{v}_0 = \mathbf{v}_0^{(\mathrm{I})}$ and $\mathbf{v}_0^{(\mathrm{II})} = 0$. The condition that nontrivial solutions exist yields the following dispersion relations:

$$\omega = \pm k C_a^{(\mathrm{II})} \cos\left(\phi_{\mathrm{II}} - \psi\right), \tag{3.15a}$$

$$\omega = k\left[V_1 \cos\psi \pm C_a^{(\mathrm{I})} \cos\left(\phi_{\mathrm{I}} - \psi\right)\right], \tag{3.15b}$$

and

$$\omega = k\frac{\rho_1}{\rho_1+\rho_2} v_0 \cos\psi \tag{3.15c}$$

$$\pm \; i\frac{k}{\rho_1+\rho_2}\left\{\rho_1\rho_2 v_0^2\cos^2\psi - (\rho_1+\rho_2)\left(\rho_1 C_a^{(\mathrm{I})2}\cos^2\left(\phi_{\mathrm{I}}-\psi\right) + \rho_2 C_a^{(\mathrm{II})2}\cos^2\left(\phi_{\mathrm{II}}-\psi\right)\right)\right\}^{1/2}$$

where $C_a^{(i)} = \left|\mathbf{B}_0^{(i)}\right| \Big/ \sqrt{\rho^{(i)}}$ $(i = \mathrm{I}, \mathrm{II})$ is the Alfvén speed of the fluid $i$, $v_0 = \left|\mathbf{v}_0^{(\mathrm{I})}\right|$, $\phi_i$ is the angle between $x$-axis and the magnetic field $\mathbf{B}^{(i)}$ $(i = \mathrm{I}, \mathrm{II})$ and $\psi$ is the angle between $x$-axis

and the propagation vector k (Fig. 5). Clearly the dispersion relations (3.15a) and (3.15b) represent stable solutions. From the dispersion relation (3.15c), we obtain the following condition of instability:

$$v_0^2 \cos^2\psi \;>\; \frac{\rho_1+\rho_2}{\rho_1\rho_2}\left(B_0^{(\mathrm{I})_2}\cos^2(\phi_{\mathrm{I}}-\psi)+B_0^{(\mathrm{II})_2}\cos^2(\phi_{\mathrm{II}}-\psi)\right), \tag{3.16a}$$

which can also be written as

$$(\mathbf{k}\cdot\mathbf{v}_0)^2 \;>\; \frac{\rho^{(\mathrm{I})}+\rho^{(\mathrm{II})}}{\rho^{(\mathrm{I})}\rho^{(\mathrm{II})}}\left(\rho^{(\mathrm{I})}\left(\mathbf{k}\cdot\mathbf{C}_a^{(\mathrm{I})}\right)^2+\rho^{(\mathrm{II})}\left(\mathbf{k}\cdot\mathbf{C}_a^{(\mathrm{II})}\right)^2\right), \tag{3.16b}$$

where $\mathbf{C}_a^{(i)} = \mathbf{B}_0^{(i)}/\sqrt{\rho^{(i)}}$ $(i = \mathrm{I}, \mathrm{II})$. When this condition is met, the instability sets in at the magnetopause. This condition tends to be satisfied near the equatorial plane of the dayside, where k is parallel to the streaming velocity $\mathbf{v}_0$ and perpendicular to the magnetic field $\mathbf{B}^{(\mathrm{II})}$ in the magnetosphere, i.e., $\psi = 0$, $\phi_{\mathrm{II}} = \pi/2$. By taking into account the fact that $\rho^{(\mathrm{I})} \gg \rho^{(\mathrm{II})}$, the foregoing condition for the Kelvin-Helmholtz instability with $\psi = 0$ and $\phi_{\mathrm{II}} = \pi/2$ becomes

$$v_0^2 > B^{(\mathrm{I})_2}\cos^2\phi_{\mathrm{I}}/\rho^{(\mathrm{II})} \tag{3.17}$$

and the growth rate $\mathrm{Im}\,\omega$ of the instability is given by

$$\mathrm{Im}\,\omega = k\left\{\left(\frac{\rho^{(\mathrm{II})}}{\rho^{(\mathrm{I})}}\right)\left(v_0^2-\frac{B^{(\mathrm{I})_2}}{\rho^{(\mathrm{II})}}\cos^2\phi_{\mathrm{I}}\right)\right\}^{1/2}. \tag{3.18}$$

We note here that the right-hand side of Eq. (3.17) represents the stabilizing effect of the magnetosheath magnetic field.

In the previous model, we did not take into account effects of finite thickness of the magnetopause. However, as shown below, waves with wavelengths comparable to the thickness of the magnetopause are significantly affected by finite thickness of the magnetopause. For example, the linear growth rate shown in Eq. (3.18) shows that a perturbation with shorter wavelength (larger $k$) has a larger growth rate. This apparent counter-intuitive large growth rate of a wave with large $k$ is reduced significantly by the sheared flow inside the magnetopause.

Ong and Roderick [1972] used the following model of a shear layer of thickness $2d$ in the $x$–$z$ plane as shown in Fig. 6. This configuration models the flow field and magnetic field on the dusk side in the equatorial plane; regime (I) and (III) represent the magnetosheath and the magnetopause, respectively, with constant magnetic fields $B_0^{(\mathrm{I})}$ and $B_0^{(\mathrm{III})}$ and constant flow field $\pm V/2$. The equilibrium magnetic field $\mathbf{B}_0$ and the mean flow field $\mathbf{v}_0$ are assumed to depend on the coordinate $y$ only as $\mathbf{B}_0 = B_{0z}(y)\mathbf{e}_z + b_0\mathbf{e}_x$ and $v_0 = v_0(y)e_x$, where $B_{0z}(y) = B_0^{(\mathrm{I})}$ for $y \geq d$, $B_{0z}(y) = B_0^{(\mathrm{III})}$ for $y \leq d$, $B_{0z}(y)$ for $|y| \leq d$ is a given arbitrary function, $b_0$ is a constant and

$$v_0(y) = \begin{cases} V/2 \\ Vy/2d \\ -V/2. \end{cases}$$

We note that there is a small component of the equilibrium magnetic field $b_0$ tangential to the flow velocity ($b_0 \ll B_{0\mathrm{II}}$). Here this system has been transformed in such a way that the mean velocity $v_0(y)$ is an odd function and the flows in regions (I) and (III) are given by $V_0/2$ and $-V_0/2$, respectively. Assuming the plasma is described by the ideal incompressible MHD equations (2.1a), (2.1b), (2.1d), (2.1e), and $\nabla \cdot \mathbf{v} = 0$, we impose a small perturbation whose time, $x$- and $z$-dependence is given by $\exp i(\omega t - k_x x - k_z z)$. We then obtain the following set of equations:

$$i\rho\omega^* v_{1x} + \rho v_{1y}\frac{d}{dy}v_0 = ik_x p_1 - iB_{0z}(k_z B_{1x} - k_x B_{1z}), \tag{3.19a}$$

$$\begin{aligned} i\rho\omega^* v_{1y} &= -\frac{d}{dy}(p_1 + B_{0z}B_{1z}) - b_0\left(\frac{dB_{1x}}{dy} + ik_x B_{1y}\right) \\ &\quad - ik_z B_{0z}B_{1y}, \end{aligned} \tag{3.19b}$$

$$i\rho\omega^* v_{1z} = ik_z p_1 + B_{1y}\frac{dB_{0z}}{dy} + ib_0(k_z B_{1x} - k_x B_{1z}), \tag{3.19c}$$

$$\frac{dv_{1y}}{dy} - ik_x v_{1x} - ik_z v_{1z} = 0, \tag{3.19d}$$

$$\frac{dB_{1y}}{dy} - ik_x B_{1x} - ik_z B_{1z} = 0, \tag{3.19e}$$

$$i\omega^* B_{1y} = -i\left(b_0 k_x + B_{0z} k_z\right) v_{1y}, \tag{3.19f}$$

$$i\omega^* B_{1z} + v_{1y}\frac{dB_{0z}}{dy} = -i\left(b_0 k_x + B_{0z} k_z\right) v_{1z}, \tag{3.19g}$$

where $\omega^* = \omega - v_0(y)k_x$ and $\rho$ is assumed to be constant. The boundary conditions are that all perturbed quantities vanish at $|y| \to \infty$. We now consider the most unstable mode which propagates in a direction perpendicular to the field ($k_z = 0$) in the region (III) or the magnetosphere [Southwood, 1968]. Using $k_z = 0$, we obtain

$$v_{1x} = -\frac{i}{k_x}\frac{dv_{1y}}{dx}, \tag{3.20}$$

$$B_{1y} = -\frac{b_0 k_x}{\omega^*} v_{1y}, \tag{3.21}$$

and

$$\begin{aligned} B_{1x} &= -\frac{i}{k_x}\frac{dB_{1y}}{dy} \\ &= ib_0\frac{d}{dy}\left(\frac{v_{1y}}{\omega^*}\right) \end{aligned} \tag{3.22}$$

from Eqs. (3.19d), (3.19f), and (3.19e), respectively. From Eq. (3.19a) and Eq. (3.20), we obtain

$$(p_1 + B_0 B_{1z}) = -i\frac{\rho\omega^*}{k_x^2}\frac{dv_{1y}}{dy} - i\rho\frac{dv_0}{dy}v_{1y}. \tag{3.23}$$

Combining Eqs. (3.19b) and (3.21)–(3.23) yields the following equation for $v_{1y}$:

$$\begin{aligned} &\omega^{*2}\left(\omega^{*2} - k_x^2 C_a^2\right)\frac{d^2 v_{1y}}{dy^2} - 2k_x^3 C_a^2\frac{dv_0}{dy}\omega^*\frac{dv_{1y}}{dy} \\ &- \left\{k_x\omega^*\left(k_x\omega^* - \frac{d^2 v_0}{dy^2}\right)\left(\omega^{*2} - k_x^2 C_a^2\right) + 2k_x^4 C_a^2\left(\frac{dv_0}{dy}\right)^2\right\} v_{1y} = 0, \end{aligned} \tag{3.24}$$

where $C_a^2 = b_0^2/\rho$. The boundary conditions of Eq. (3.24) are given by $v_{1y} \to 0$ as $|y| \to \infty$. We note that the function $B_{0z}(y)$ does not enter Eq. (3.24). The mean magnetic field component $B_{0z}$ perpendicular to the direction of the wavenumber vector and the mean flow velocity does not affect the stability in the incompressible flow case. This independence

of the stability on the perpendicular magnetic field is also known for the case of a zero-thickness shear layer with a constant perpendicular magnetic field [Chandrasekhar, 1961]. Equation (3.24) can be significantly simplified with the use of new variable

$$\delta(y) = v_{1y}(y)/\omega^*.$$

With this new variable $\delta$, Eq. (3.19) is transformed to

$$\frac{d}{dy}\left\{\left(\omega^{*2}(y) - k_x^2 C_a^2\right)\frac{d\delta}{dy}\right\} + \left(\omega^{*2}(y) - k_x^2 C_a^2\right)\delta = 0, \tag{3.25}$$

with the boundary conditions $\delta(y) \to 0$ as $|y| \to \infty$. To simplify Eq. (3.25) further, we also define a new dependent variable $\xi$ by

$$\xi = k_x y - \Omega$$

with $\Omega = \omega d/V$. In the regions I and III, where $\omega^* = \omega - k_x v_0(y)$ is constant, Eq. (3.25) may be written in terms of $\xi$ as

$$\frac{d^2\delta}{d\xi^2} + \delta = 0.$$

The solution of this equation in the region I ($\xi \geq k_x d - \Omega$) is given by

$$\delta = A_1 \exp(-\xi) \qquad (\xi \geq k_x d - \Omega) \tag{3.26}$$

and the solution in the region III ($\xi \leq -k_x d - \Omega$) is given by

$$\delta = A_3 \exp(\xi) \qquad (\xi \leq -k_x d - \Omega)\,. \tag{3.27}$$

Here $A_1$ and $A_3$ are constants. In the region II, Eq. (3.24) becomes

$$\frac{d}{d\xi}\left\{\left(\xi^2 - \alpha^2\right)\frac{d\delta}{d\xi}\right\} - \left(\xi^2 - \alpha^2\right)\delta = 0, \tag{3.28}$$

where

$$\alpha = \left|\frac{k}{A}\right|$$

$$k = k_x d$$

$$A^2 = \frac{V^2}{C_a^2}.$$

We now solve Eq. (3.28) by means of the WKB method. For the range of the variable $\xi$ such that $\xi^2 - \alpha^2 \neq 0$, we transform $\xi$ to

$$\eta = \frac{1}{2\alpha} \log \left| \frac{\xi - \alpha}{\xi + \alpha} \right|,$$

and therefore we have

$$d\eta = \frac{d\xi}{\xi^2 - \alpha^2}.$$

Then Eq. (3.22) is transformed to

$$\frac{d^2\delta}{d\eta^2} - \left(\xi^2(\eta) - \alpha^2\right)^2 \delta = 0. \tag{3.29}$$

For $\xi^2$ not near $\alpha^2$, the WKB method yields the asymptotic solution of Eq. (3.29) in terms of $\xi$ as

$$\delta = A_+ \left(\xi^2 - \alpha^2\right)^{-1/2} \exp \xi + A_- \left(\xi^2 - \alpha^2\right)^{-1/2} \exp(-\xi). \tag{3.30}$$

The boundary conditions to be applied at $z = \pm d$ are that the normal velocity $v_{1y}(y)$ and the normal component of the stress $p_1 + B_0 B_{1z}$ be continuous. Since $\omega^*(y) = \omega - k_x v_0(y)$ is continuous at $z = \pm d$, the continuous normal velocity conditions are

$$[\delta]_{z=\pm d} = 0, \tag{3.31}$$

where $[\quad]_z$ indicates the change in the value of the enclosed quantity across the discontinuity surface at $z$. Since Eq. (3.23) may be written as

$$(p_1 + B_0 B_{1z}) = -i \frac{\rho \omega^{*2}}{k_x} \frac{d\delta}{dy},$$

the continuous normal stress conditions are given by

$$\left[\frac{d\delta}{d\xi}\right]_{\xi=\pm k-\Omega} = 0. \tag{3.32}$$

Equation (3.32) may also be obtained by the integration of Eq. (3.28) across the interfaces at $\xi = \pm k_z d - \Omega = \pm k - \Omega$. Equations (3.31) and (3.32) give the following four homogeneous

equations for $A_1$, $A_+$, $A_-$, $A_3$:

$$\begin{aligned}
\mathcal{A}_1 + \mathcal{A}_+ e^k + \mathcal{A}_- e^{-k} &= 0, \\
\mathcal{A}_3 + \mathcal{A}_+ e^{-k} + \mathcal{A}_- e^k &= 0, \\
\mathcal{A}_1 + \mathcal{A}_+ \left( \frac{\xi_1}{\xi_1^2 - \alpha^2} - 1 \right) e^k + \mathcal{A}_- \left( \frac{\xi_1}{\xi_1^2 - \alpha^2} + 1 \right) e^{-k} &= 0, \\
\mathcal{A}_3 - \mathcal{A}_+ \left( \frac{\xi_2}{\xi_2^2 - \alpha_2} - 1 \right) e^{-k} - \mathcal{A}_- \left( \frac{\xi_2}{\xi_2^2 - \alpha_2} + 1 \right) e^k &= 0.
\end{aligned}$$

Here

$$\begin{aligned}
\mathcal{A}_1 &= -\frac{d\sqrt{\xi_1^2 - \alpha^2}}{(\Omega - k)V} e^{-k} A_1, \\
\mathcal{A}_3 &= -\frac{d\sqrt{\xi_2^2 - \alpha^2}}{(\Omega + k)V} e^{-k} A_3, \\
\mathcal{A}_+ &= e^{-\Omega} A_1, \\
\mathcal{A}_- &= e^{-\Omega} A_2, \\
\xi_1 &= k - \Omega, \\
\xi_2 &= -k - \Omega.
\end{aligned}$$

The condition that the equations above have nontrivial solution $\mathcal{A}_1$, $\mathcal{A}_+$, $\mathcal{A}_-$, $\mathcal{A}_3$ gives the dispersion relation

$$\begin{aligned}
&\Omega^4 + \Omega^2 \left[ k - 2k^2 \left( 1 + \frac{1}{A^2} \right) - \frac{1}{4} \left( 1 - \exp(-4k) \right) \right] \\
&+ k^4 \frac{(A^2 - 1)^2}{A4} - k^3 \frac{A^2 - 1}{A^2} + \frac{1}{4} k^2 \left( 1 - \exp(-4k) \right) = 0,
\end{aligned} \tag{3.33}$$

where $\Omega = 2\omega d/V$ and $k = k_x d$. Figure 7 shows this dispersion relation compared to the dispersion relation of the zero thickness magnetopause. It is clear that the growth rate of perturbations with large $k$ is significantly reduced by the effect of the finite thickness of the magnetopause and there is a critical $k_c$ such that any waves with $k > k_c$ are stable.

In this section, we have reviewed the basic theory of the Kelvin-Helmholtz instability at the magnetopause. The compressibility effect on this instability in the case of finite thickness of the magnetopause is also discussed by Ong and Roderick [1972] and it is shown that the compressibility effect does not alter the dispersion relation Eq. (3.33) significantly. The required condition, Eq. (3.17), for the Kelvin-Helmholtz instability obtained under the assumption of zero thickness of the magnetopause (which gives more unstable waves than the condition obtained under the assumption of finite thickness), however, is not easy to satisfy [Hasegawa and Sato, 1989]. For example, with $B_1 = 20\gamma$, $\rho_2/(\text{proton mass}) = 0.1\,\text{cm}^{-3}$ and $\phi_1 = 0$, then $V_1 > 2 \times 10^3$km/s, which is rather large for the solar wind [Nishida, 1978]. Therefore more effort is needed to determine a significant agent of wave generation, not only considering the Kelvin-Helmholtz instability in a more realistic configuration of the magnetopause but also taking into account other effects such as dayside reconnection.

# 4. Summary and Discussion

In this review, we have focused on Alfvén resonance of geomagnetic field lines and Kelvin-Helmholtz instability at the magnetopause as a possible mechanism of the long-period magnetic pulsations (pc3 $\sim$ pc5). In Sec. 2, we discussed the theory of resonant excitation of the Alfvén wave at a particular geomagnetic field line, where the compressional wave from an outside source is converted to the shear Alfvén wave due to the nonuniformity of the magnetic field. In Sec. 3, based on the incompressible MHD model, the dispersion relations of the wave on the magnetopause are derived under the assumptions of the zero thickness and the finite thickness of the magnetopause. It is shown therein that finite thickness of the layer with shear of the magnetic field and streaming velocity stabilizes the short wavelength perturbations which are unstable in the zero thickness analysis. In these theoretical treatments, effects of magnetic field curvature are not taken into account. Despite such idealization of the models, however, it is believed that essential physical mechanisms of the

magnetic pulsations are contained in the theories presented in this review.

Apart from the curvature effects, we now discuss briefly some other effects, particularly on the Kelvin-Helmholtz instability. Fejer [1964] and Sen [1964, 1965] discussed effects of compressibility on the Kelvin-Helmholtz instability, simplifying the problem in different ways, and drew different conclusions. Fejer finds the most unstable modes propagate parallel to the streaming velocity while Sen finds the most unstable modes propagate perpendicular to the unperturbed magnetic field. The relationship of these conclusions is discussed by Southwood [1968] in a more general treatment. Both Sen and Fejer, however, find in their compressible MHD models that there is an upper limit of the streaming velocity for each normal mode solution. With the streaming velocity larger than this upper limit, the Kelvin-Helmholtz instability is stabilized. This upper limit of the streaming velocity, which does not exist in the incompressible model, seems to have little physical significance in the actual stability problem since it is always possible to choose a direction of the wavenumber in such a way that there exists an unstable mode [Southwood, 1968]. Effects of more realistic configurations of the magnetosheath-magnetosphere boundary are also discussed by several authors. For example, Lee, Albano, and Kan [1981] studied the model which consists of three uniform plasma regions: the magnetosheath, the boundary layer, and the magnetosphere. The middle layer of the uniform plasma, as a matter of fact, represents a boundary layer inside and adjacent to the magnetopause, rather than the magnetopause itself. This boundary layer consists of a plasma with nearly similar temperature and flow properties to the solar wind on the magnetosheath due to permeability of the magnetopause [Haerendel and Paschmann, 1982]. Lee, Albano, and Kan find that there are two unstable modes in the magnetopause boundary region: one is excited at the magnetosheath-boundary layer interface (the magnetopause mode) and the other is excited at the inner surface of the boundary layer (the inner mode). While the magnetopause mode can be stabilized by the magnetic field in the magnetosheath, the inner mode is found to be unstable most of the time. Figure 6 schemat-

ically shows the inner mode at the interface between the magnetosphere and the boundary layer.

Recently Wolfe et al. [1988] discussed the penetration of the magnetopause mode and the inner mode deep into the magnetosphere. It is observed that the monochromatic surface waves generated at the magnetopause have sufficient amplitude deep inside the magnetosphere to cause a field line resonance. As first pointed out by Lanzerotti et al. [1981], the lack of understanding of the mechanism for the evanescent waves to have such large decay lengths in the magnetosphere was a major difficulty in describing the long-period magnetic pulsations self-consistently. It is found by Wolfe et al. [1988], however, that the inner mode may have its energy reduced by only one order of magnitude over a penetration depth of about $8R_E$ under some conditions while the magnetopause mode always has extremely small decay length ($\sim 1R_E$) regardless of the thickness of the boundary layer. Thus taking into account the finite size of the magnetosheath-magnetosphere boundary layer and the associated inner mode may yield a more self-consistent picture of the long-period magnetic pulsations.

## Acknowledgements

The authors would like to thank Eliezer Hameiri, G. S. Lakhina, and Akira Hasegawa for many helpful discussions. This work was supported by Air Force Office of Scientific Research under Grant No. AFOSR-86-0167.

# References


Chen, L., and A. Hasegawa (1974a). J. Geophys. Res., **79**, 1024.

Chen, L., and A. Hasegawa (1974b). J. Geophys. Res., **79**, 1033.

Chandrasekhar, S. (1961). Hydrodynamic and Hydromagnetic Stability, Oxford University Press, Oxford.

Fejer, J. A. (1964). Phys. Fluids, **7**, 499.

Grossmann, W., and J. Tataronis (1973). Z. Physik, **261**, 217.

Haerendel, E., and G. Paschmann (1982). Interaction of the Solar Wind with the Dayside Magnetosphere, in *Magnetospheric Plasma Physics* (ed. by A. Nishida, Center for Advanced Publication Japan, Tokyo).

Hameiri, E., and J. H. Hammer (1979). Phys. Fluids, **22**, 1700.

Hasegawa, A., and L. Chen (1974). Space Sci. Rev., **16**, 347.

Hasegawa, A., and T. Sato (1989). *Space Plasma Physics 1. Stationary Processes*, (Springer-Verlag, New York).

Hirasawa, T. (1970). Rep. Ionos. Space Res. Jap., **24**, 66.

Hones, E. W., J. Birn, S. J. Bame, J. R. Asbridge, G. Paschmann, N. Sckopke, and G. Haerendel (1981). J. Geophys. Res., **86**, 814.

Lanzerotti, L. J., H. Fukunishi, A. Hasegawa, and L. Chen (1973). Phys. Rev. Lett., **31**, 624.

Lanzerotti, L. J., and D. J. Southwood (1979). Hydromagnetic Waves, in *Solar System Plasma Physics.* Vol. III, (ed. by L. J. Lanzerotti, C. F. Kennel, and E. N. Parker, North-Holland, Amsterdam).

Lee, L. C., R. K. Albano, and J. R. Kan (1981). J. Geophys. Rev., **86**, 54.

Nishida, A. (1978). *Geomagnetic Diagnosis of the Magnetosphere*, (Springer-Verlag, New York).

Ong, R. S. B., and N. Roderick (1972). Planet. Space Sci. **20**, 1.

Rostoker, G. (1979). Fund. Cosmic Phys., **4**, 211.

Saito, T., T. Sakurai, and Y. Koyama (1976). J. Atmosph. Terrest. Phys., **38**, 1265.

Samson, J. C., J. A. Jacobs, and G. Rostoker (1971). J. Geophys. Res., **76**, 3675.

Samson, J. C., and G. Rostoker (1972). J. Geophys. Res., **77**, 6133.

Schulz, M., and L. J. Lanzerotti (1974). *Particle Diffusion in the Radiation Belts*, (Springer-Verlag, New York).

Sen, A. K. (1963). Phys. Fluids, **6**, 1154.

Sen, A. K. (1964). Phys. Fluids, **7**, 1293.

Sen, A. K. (1965). Planet. Space Sci., **13**, 131.

Southwood, D. J. (1968). Planet. Space Sci., **16**, 587.

Stewart, B. (1861). Phil. Trans. Roy. Soc. London, PP423.

Tataronis, J., and W. Grossmann (1973). Z. Physik, **261**, 203.

Wolfe, A., private communication (1988).

| Name | Frequency | Name | Period or Rise Time |
|---|---|---|---|
| SHF | 3—30 GHz | Pc 1 | $2\pi/\omega = 0.2—5.0$ sec |
| UHF | 0.3—3.0 GHz | Pc 2 | $2\pi/\omega = 5—10$ sec |
| VHF | 30—300 MHz | Pc 3 | $2\pi/\omega = 10—45$ sec |
| HF | 3—30 MHz | Pc 4 | $2\pi/\omega = 45—150$ sec |
| MF | 0.3—3.0 MHz | Pc 5 | $2\pi/\omega = 150—600$ sec |
| LF | 30—300 kHz | | |
| VLF | 3—30 kHz | Pi 1 | $\tau_r = 1—40$ sec |
| ELF | 3—3000 Hz | Pi 2 | $\tau_r = 40—150$ sec |
| ULF | $\lesssim 3$ Hz | sc. si | $\tau_r \sim 300$ sec |

Classification of magnetospheric signals (after Shultz and Lanzerotti, 1974).

TABLE 1

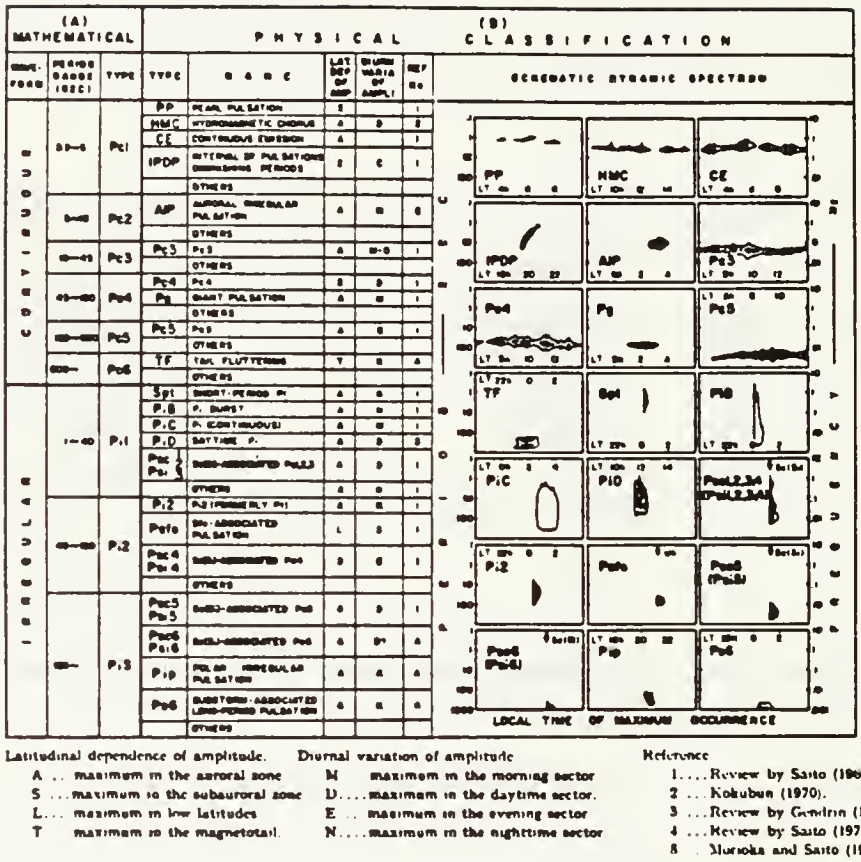


Classification of magnetic pulsations (after Saito et al., 1976).

TABLE 2

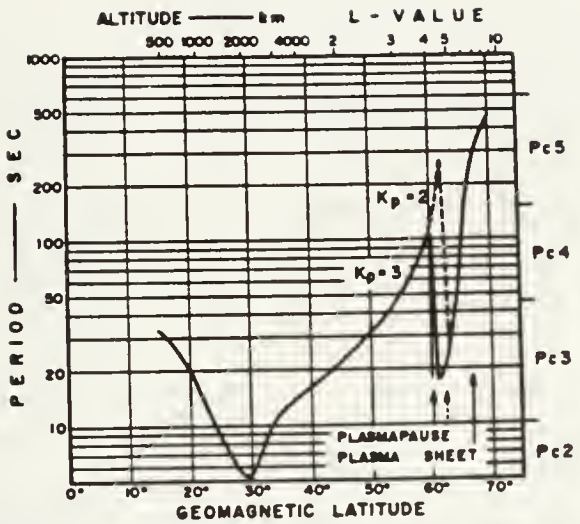


Fundamental period $T$ of the magnetic field oscillation given by Eq. (1.1). The dipole magnetic field is assumed, where field lines are labeled by the geomagnetic latitude of their intersection with the earth or by the equatorial crossing distance ($L$-value) (after Saito et al., 1976).

FIGURE 1

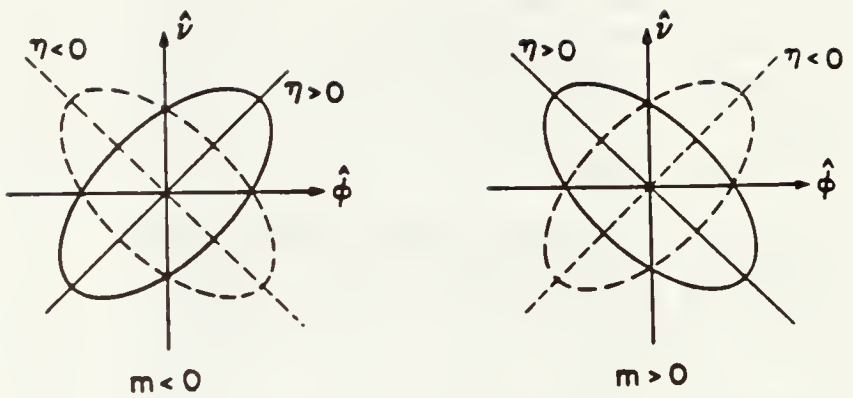


Tilt of the major axis near the resonant field line at the equatorial plane (after Hasegawa and Chen, 1974).

FIGURE 2

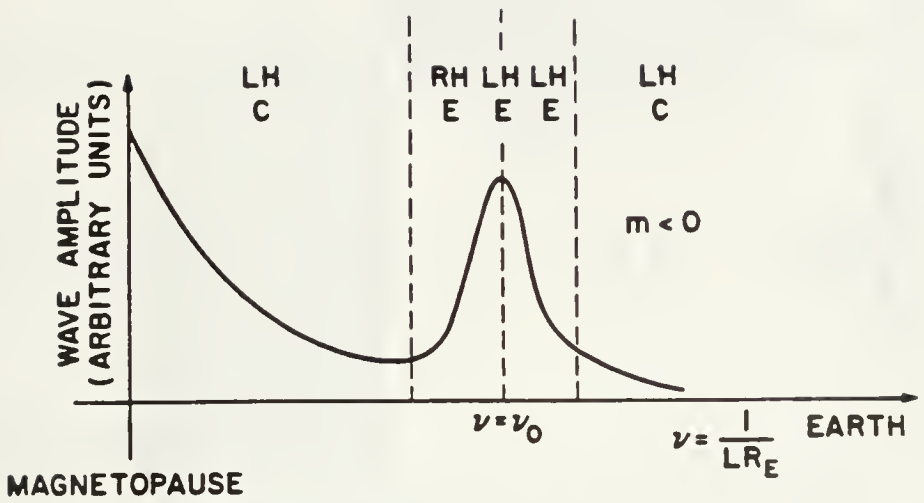


Schematic diagram of the wave amplitude and sense of polarization vs. radius in the equatorial plane for the local morning. When projected along the field lines to the ground, it can be viewed as a function of the latitude. C and E stand for circular and elliptical polarization, respectively, and $\nu_0$ is the location of the resonant field line (after Hasegawa and Chen, 1974).

FIGURE 3

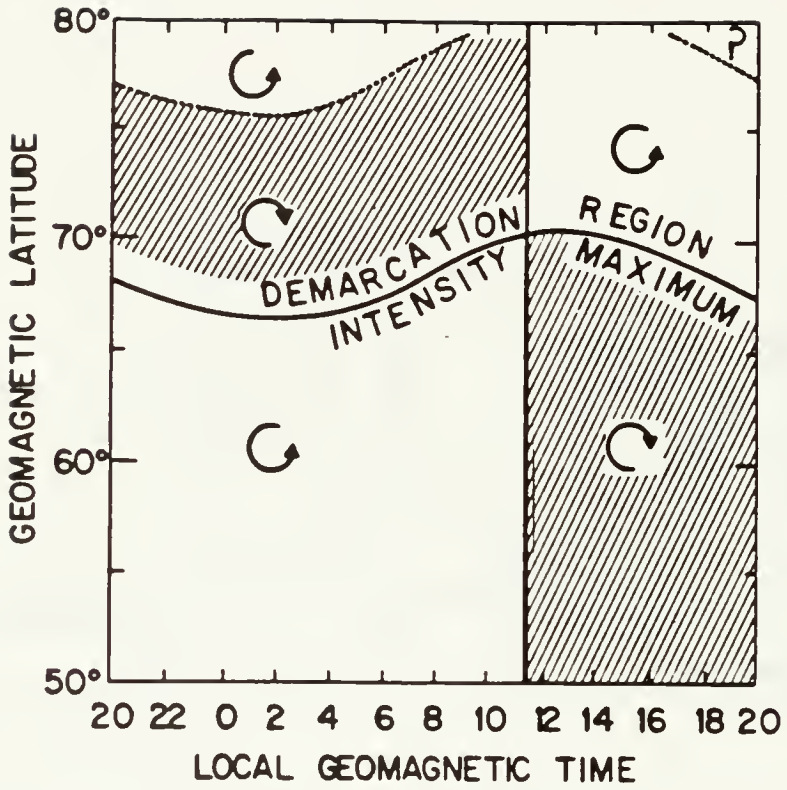


The diurnal variation of the sense of polarization for quasi-monochromatic pulsation (frequency $\simeq 5\,\mathrm{mHz}$) (after Samson et al., 1971).

FIGURE 4

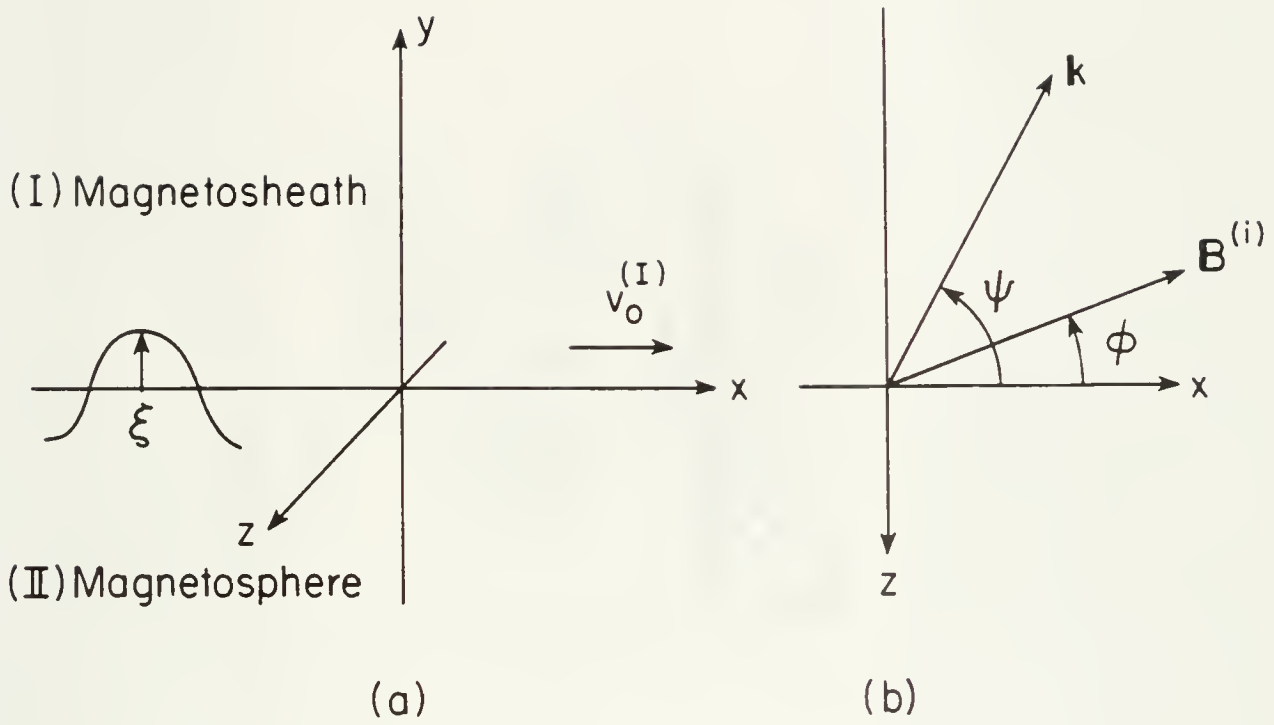


Coordinate system of the problem (a) the unperturbed magnetopause is the $x$–$z$ plane. (b) the definition of the angles $\phi$ and $\psi$ (modified after Sen, 1963).

FIGURE 5

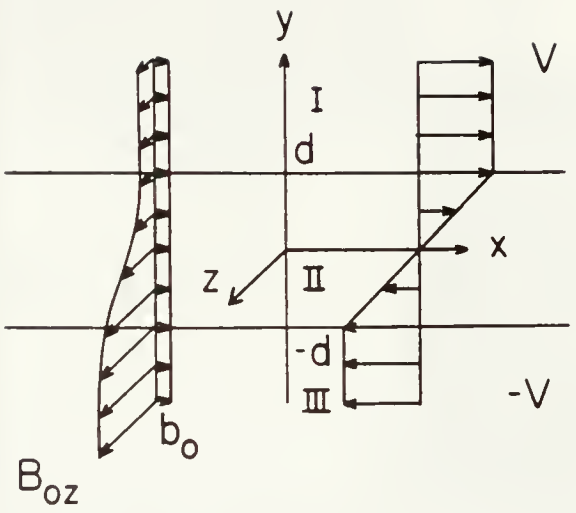


Shear layer model (modified after Ong and Roderick, 1972).

FIGURE 6

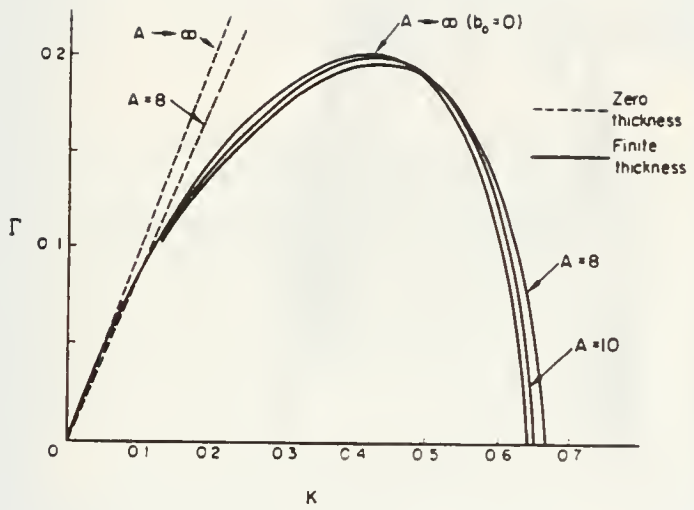


Growth rate vs. wavenumber in the case where finite thickness of the magnetopause is taken into account (after Ong and Roderick, 1972).

FIGURE 7

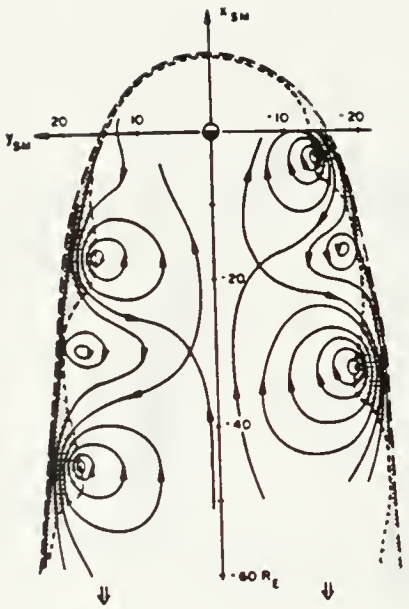


Schematic interpretation of the inner mode. The shaded area is the boundary layer and its wavy inner edge is indicated by the dotted line (after Hones et al., 1981).

FIGURE 8

NYU MF- 120
Hamaguchi, Satoshi
Theory of long-period
magnetic pulsations.
c.1

| DATE DUE | BORROWER'S NAME |
|---|---|
| | |
| | |
| | |
| | |